BEAM IMAGING OF A HIGH-BRIGHTNESS ELLIPTIC ELECTRON GUN*

T.M. Bemis[a], C. Chen[a,b], M.H. Lawrence[a] and J. Zhou[a]
[a)]Beam Power Technology, Inc., Chelmsford, MA 01824, U.S.A.
[b)]MIT, Cambridge, MA 02139, U.S.A

Abstract

An innovative research program is being carried out to experimentally demonstrate a high-brightness, space-charge-dominated elliptic electron beam using a non-axisymmetric permanent magnet focusing system. Results of the fabrication, initial testing and beam imaging of an elliptic electron gun are reported. Good agreement is found between the experimental measurements and simulation.

INTRODUCTION

A high-brightness elliptic beam [1-4] is a novel device which has many applications. Once developed, a large-aspect-ratio elliptic electron beam will enable the development of L-band elliptic-beam klystrons (EBKs) or sheet-beam klystrons (SBKs) [5-6], which are more efficient and lower voltage than multi-beam klystrons (MBKs) for the International Linear Collider (ILC). In addition, high-brightness elliptic charged-particle (electron, muon, proton, antiproton, and ion) beams have wide applications in other accelerators for nuclear physics research and high-energy density physics research because they are naturally matched to alternating-gradient focusing systems where the transverse section of the beam is a pulsating ellipse [7]. Furthermore, high-aspect-ratio elliptic beams will enable the research and development of advanced accelerators with planar structures [8,9].

This paper reports on the progress in an on-going experimental demonstration of a high-brightness space-charge-dominated elliptic electron beam operating at 2290 V with a perveance of 1.0×10^{-6}. In particular, results of the fabrication, initial testing, and beam imaging of the elliptic thermionic electron gun are reported. Good agreement is found between theory, simulation and experimental measurements.

DESIGN OF ELLIPTIC ELECTRON GUN

The elliptic electron gun was based on the concept design in [2,3]. Results of fabrication and testing were reported in [10]. Results of a first beam imaging experiment were reported in [11].

The parameters for the elliptic electron gun are listed in Table 1. The perveance of the elliptic electron gun is $I_b/V_b^{3/2}=1.0\times 10^{-6}$.

* Supported by Department of Energy, Grant No. DE-FG02-07ER84910. The basic gun design was also supported, in part, by Department of Energy, Grant No. DE-FG02-95ER40919, Air Force Office of Scientific Research, Grant No. FA9550-06-1-0269 and the MIT Deshpande Center.

Table 1: Design Parameters of Elliptic Electron Gun

Parameter		Value
Beam Current	I_b	0.11 A
Beam Voltage	V_b	2290 V
Major Semiaxis	a	0.373 cm
Minor Semiaxis	b	0.0622 cm
Diode A-K Gap	d	0.411 cm

BEAM IMAGING EXPERIMENT

Capturing images of the beam as it exits the gun was accomplished by placing a phosphor screen in front of the anode aperture opening. Beam cross sectional images were captured by photographing the projected green light generated by electrons as they hit the screen. The phosphor screen was made using 10-15 microns of P-43 phosphor (Gd_2O_2S:Tb) on an indium tin oxide (ITO) coated glass disk. The decay time of the screen is 1 ms.

Fig. 1 shows a schematic of the beam imaging system. The plane of the phosphor screen is 15.6 mm from the cathode emitting surface.

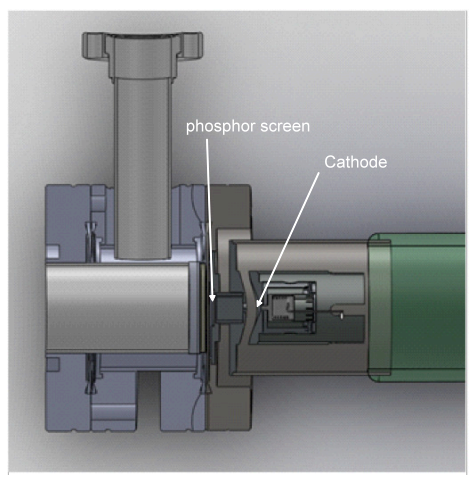

Figure 1: SOLIDWORKS drawing of the fixed beam diagnostic system. The vac-ion pump is attached to the vertical conflat flange connector on the left. The plane of the phosphor screen is 15.6 mm to the left of the plane of the cathode.

In order to prevent damage to the screen from overheating, the beam was pulsed. Care was taken to increase power incrementally, with the first set of images

taken at 900 V, and then the voltage was gradually increased until the full design voltage of 2290 V was achieved.

The electron gun was pulsed with both 100 ns pulses at 10 Hz and 1 μs pulses at 1 Hz. Typical rise and fall times of the voltage pulses were about 100 ns. Because the phosphor screen was damaged when longer pulses were applied at 2290 V, we report only the results taken at a beam voltage of 900 V in the remainder of this paper.

For the data taken at the beam voltage of 900 V, the heat current for the cathode was set at 1.8 A, which was at the onset of space-charge-limited emission according to the roll-off data taken earlier [10]. The cathode temperate was 1000° C.

The digital photograph in Fig. 2 shows an image of a 1 μs-long beam on the phosphor screen at 900 V as it exits the anode aperture and expands (in the absence of an applied magnetic focusing field). The green spot is the electron beam, whereas the red shading surrounding the beam image is radiant heat from the cathode.

The intensity on the digital photograph as measured in terms of a grey scale is approximately proportional to the time-integrated beam current density (beam density) over the 1 μs beam pulse. Fig. 3 shows plots of the intensity versus the horizontal and vertical positions, respectively. The data in Fig. 3 include both the signal and background. While a detailed data analysis remains to be carried out, it should be noted that the plateau profile of intensity in Fig. 3 suggests a plateau-shaped beam density profile, which is a characteristic of a high-brightness, space-charged-dominated elliptic beam [12,13].

COMPARISON BETWEEN SIMULATION AND EXPERIMENT

The experiment was simulated in OMNITRAK, as shown in Fig. 4. A cross section from the OMNITRAK model shows the beam image at $z = 15.6$ mm. Note that both the OMNITRAK cross section and the photograph of the beam show triangularization of the beam. This triangularization is the result of image charge forces from the $10.74\ \text{mm} \times 7.0\ \text{mm}$ rectangular beam tunnel. The triangularization will be eliminated when the magnetic focusing field is introduced.

Table 2 shows the comparison between the full horizontal and vertical widths of the beam shape from the OMNITRAK simulation and the corresponding full widths at the half maximum of the beam intensity shown in Fig. 3. Agreement between the simulation and the experiment is within 7%, which is good.

CONCLUSION AND DISCUSSION

A research and development program is being carried out to experimentally demonstrate an elliptic electron beam using a non-axisymmetric permanent magnet focusing system and an elliptic electron gun to verify recent inventions and theoretical studies in the generation and transport of elliptic charged-particle beams. Results of the fabrication and initial beam imaging experiment of the elliptic electron gun were presented. Good agreement was found between the experimental measurements and simulation.

The experiment on the elliptic electron gun reported in this paper was performed without the magnetic focusing

Figure 2: Digital photograph of a 1 μs beam pulse taken during an operation at a repetition rate of 1 Hz.

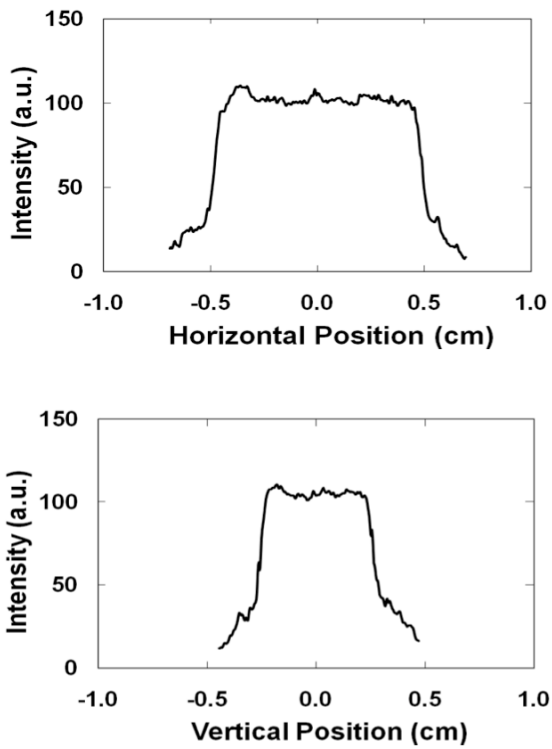

Figure 3: Intensity as measured on a grey scale in the pixels in the digital photograph shown in Fig. 2.

Table 2: Comparison between Simulation and Experiment

Parameter	Simulation	Experiment
Full horizontal beam width	10.6 mm	9.9 mm
Full vertical beam width	5.2 mm	5.4 mm

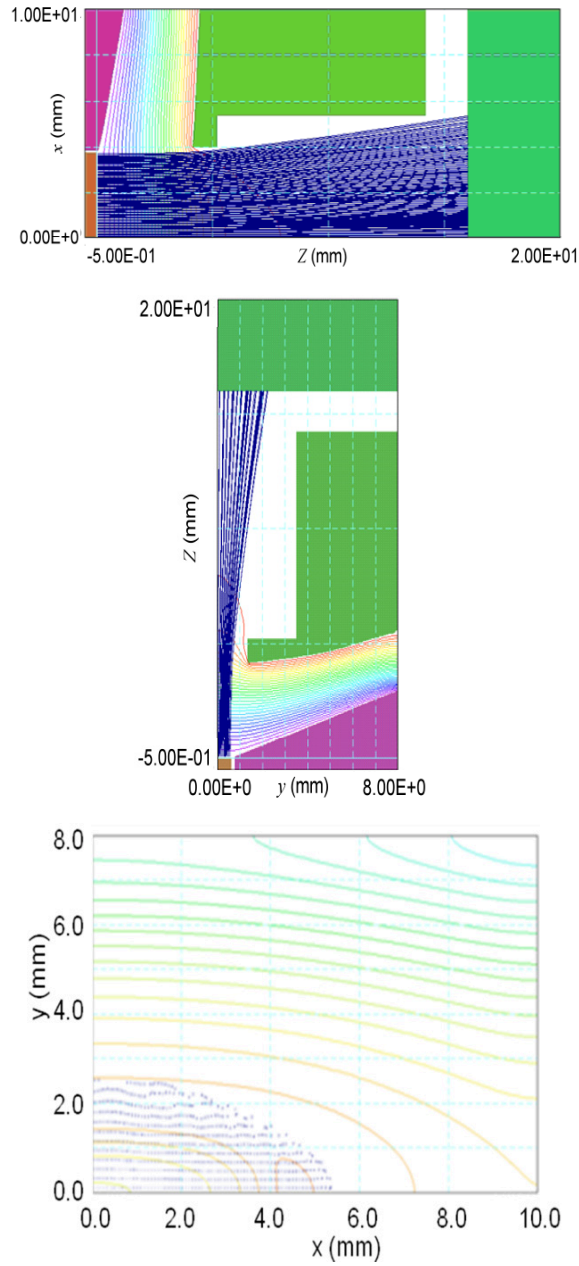

Figure 4: OMNITRAK simulation of the fixed imaging experiment with the elliptic electron gun at 900 V: a) cut plane at $y = 0$ (top); b) cut plane at $x = 0$ (middle), and c) beam cross section at $z = 15.6$ mm (bottom).

field. The magnetic focusing stack is currently under construction.

The full beam imaging experiment is being prepared which will enable images of the magnetically focused beam to be taken at various points along its length, using a moveable phosphor screen placed inside the beam tunnel.

ACKNOWLEDGMENTS

The authors wish to thank Marc Curtis, Kim Gunther and Dave Saia at Heat Wave Labs, Inc. for their assistance on hardware fabrication and experimental setup, Santiago Bernal, Ramie Kishek, Patrick O'Shea, and David Sutter at the University of Maryland Electron Ring for their guidance on the beam imaging experiment, and Wei Gai at Argonne National Laboratory for his encouragement.

REFERENCES

[1] R. Bhatt, and C. Chen, Phys. Rev. ST - Accel. Beams 8, 014201 (2005).
[2] R. Bhatt, T. Bemis and C. Chen, Proc. 2005 Part. Accel. Conf. (2005), p. 3372.
[3] R. Bhatt, T. Bemis and C. Chen, IEEE Trans. Plasma Sci. **34**, 187 (2006).
[4] R.J. Bhatt, C. Chen and J. Zhou, "Non-Axisymmetric Charged-Particle Beam System," US Patent No. 7,612,346, November 3, 2009.
[5] D. Sprehn, A Hasse, A. Jensen, E. Jongewaard, and D.Martin, Proc. 2010 Int. Part. Accel. Conf. (2010), p. 4023.
[6] A.E. Brainerd, C. Chen and J. Zhou, J. Appl. Phys. 106, 023310 (2009).
[7] C. Chen, R. Pakter, and R.C. Davidson, Nucl. Instrum. Methods **A464**, 518 (2001).
[8] L. Xiao, W. Gai and X. Sun, Phys. Rev. **E65**, 016505 (2001).
[9] B.E. Carlsten, et al., Phys. Rev. ST - Accel. Beams **8**, 062002 (2005).
[10] T. Bemis, M. Lawrence, J. Zhou and C. Chen, Proc. 2009 Part. Accel. Conf., WE6RFP056 (2009).
[11] J. Zhou, T.M. Bemis, C. Chen and M.H. Lawrence, in *Advanced Accelerator Concept*, AIP Conf. Proc. **1299**, 528 (2010).
[12] K. R. Samokhvalova, J. Zhou, and C. Chen, Phys. Plasmas **16**, 043115 (2009).
[13] C. Chen, "Adiabatic thermal beam equilibrium in periodic focusing fields," Paper WEP073 in this proceeding (2011).